

MAGNETIC EFFECTS IN GLOBAL STAR FORMATION

M.-M. Mac Low¹

RESUMEN

Hago una revisión de los efectos de los campos magnéticos en la formación estelar en galaxias. Ésto incluye los efectos de las inestabilidades magneto-rotacional (MRI por sus siglas en inglés) a escalas galácticas, magneto-Jeans, de columpio y de Parker, así como los efectos de los campos magnéticos en la evolución de la turbulencia forzada por supernovas. Argumentaré que actualmente la turbulencia mantenida principalmente por la MRI parece ser el proceso más importante para regular el proceso de formación estelar.

ABSTRACT

I review the effects of magnetic fields on star formation in galaxies. This includes the effects of the magnetorotational instability (MRI) at galactic scales, magneto-Jeans and swing instabilities, Parker instabilities, and the effects of magnetic fields on the evolution of supernova-driven turbulence. I argue that currently turbulent support by the MRI appears likely to be the most important of these processes to regulating star formation.

Key Words: magnetic fields — stars: formation — ISM: magnetic fields — galaxies: magnetic fields

1. GLOBAL STAR FORMATION

The question of what regulates star formation in galaxies remains unsolved, with at least four main scenarios, and a number of variations on some of them. To understand the role of magnetic fields, we must first briefly review these ideas.

The first is that global star formation is primarily controlled by gravitational instability of the available gas in the disk. Whether this instability is global, controlled by the combined potential of the gas and stars Rafikov (2001), or local, controlled by the behavior of individual GMCs, is still argued. The basic idea of global instability was described by Elmegreen (2002), and supported by numerical models (Krautsov 2003; Li et al. 2005a). Observational evidence for a direct correlation between star formation rate and gravitational instability in the LMC is given by Yang et al. (2007). Local instability in molecular clouds has been argued to be the rate limiting step by Krumholz (2005).

A second idea recently elucidated by Shu et al. (2007) is that magnetic regulation dominates star formation. The results of Kim & Ostriker (2006) and Shetty & Ostriker (2006) establish that the magnetic field can control the morphology of star formation in spiral galaxies. The suggestion is then made by Shu et al. (2007) that the rate limiting step in star formation is the accumulation of sufficient mass to form a supercritical cloud.

Star formation controlled by a threshold column density has been advocated by Schaye (2004). He argues that gas above the threshold will be able to cool quickly by forming molecules, which will drive gravitational instability. However, this would predict uniformly high molecular fractions at the critical column density, contrary to the observations of Martin & Kennicutt (2001).

Finally, self-regulated star formation remains on the table (e.g. Silk 1997). In this scenario, the supernovas produced by star forming regions determine the level of turbulence in the surrounding gas (e.g., Slyz et al. 2005), which determines its level of gravitational instability and thus how many stars it can form. Less star formation lowers the level of turbulence, which in turn increases the star formation rate. However, this cannot explain the lack of star formation far from star forming regions and massive stars, e.g. in the outer disks of normal galaxies, or in low surface brightness galaxies.

2. GRAVITATIONAL INSTABILITY

Global disk instability models postulate that star formation happens wherever gravitational instability (Gammie 1992; Rafikov 2001) of the combined collisionless stars (Toomre 1964) and collisional gas (Goldreich & Lynden-Bell 1965) in the disk sets in during the collapse of disk galaxies. For a gas disk, the criterion for instability is

$$Q_g \equiv \frac{\kappa c_g}{\pi G \Sigma_g} < 1, \quad (1)$$

where κ is the epicyclic frequency, c_g the speed of sound, and Σ_g the surface density of the gas disk.

¹Department of Astrophysics, American Museum of Natural History, New York, NY, 10024-5192, USA (mordecai@amnh.org).

For a collisionless stellar disk, the equivalent criterion is

$$Q_s \equiv \frac{\kappa \sigma_s}{\pi G \Sigma_s} < 1.07, \quad (2)$$

where σ_s is the stellar velocity dispersion in the radial direction, and Σ_s is the surface density of the stellar disk. [Note that following Rafikov (2001) we use a factor of π in the definition of Q_s rather than 3.36, shifting the instability criterion to slightly higher value.] Define the dimensionless quantities $q = k\sigma_s/\kappa$ and $R = c_g/\sigma_s$. Then the instability criterion for the combined disk of gas and stars is given by

$$\frac{2}{Q_s} \frac{1}{q} \left[1 - e^{-q^2} I_0(q^2) \right] + \frac{2}{Q_g} R \frac{q}{1 + q^2 R^2} > 1, \quad (3)$$

where I_0 is the Bessel function of order 0. The central determining factor in global disk instability models is then the magnitude of the turbulent support of gas.

This support cannot come solely from star formation, however. The 21 cm observations of Petric & Rupen (2007) represent the highest-resolution observation of velocity dispersion across a galactic disk, in this case that of NGC 1058. (see Figure 1).

This suggests to me that the velocity dispersion of the gas must be determined by physics more or less independent of star formation. Star formation might then be simply the response of the turbulent gas disk to gravity, depending on the amount of gas available from smooth or lumpy accretion.

What is the physical mechanism driving the turbulence? Mac Low (1999, 2003) estimates the dissipation rate for a supersonic turbulent flow to be

$$\begin{aligned} \dot{e} &= -\frac{1}{2} \frac{\rho v_{\text{rms}}^3}{\lambda_D} \\ &\simeq -(3 \times 10^{-27} \text{erg cm}^{-3} \text{s}^{-1}) \times \\ &\times \left(\frac{n}{1 \text{cm}^{-3}} \right) \left(\frac{v_{\text{rms}}}{10 \text{km s}^{-1}} \right)^3 \left(\frac{\lambda_D}{100 \text{pc}} \right)^{-1}, \end{aligned} \quad (4)$$

where ρ is the average density, v_{rms} the rms velocity, and λ_D the effective driving scale of the turbulence. Note in particular the cubic dependence of the required energy input on the rms velocity. A factor of two reduction in the velocity will lead to an order of magnitude lower energy requirement.

Sellwood & Balbus (1999) suggested that the magnetorotational instability (MRI) (Balbus & Hawley 1991, 1998) can drive significant turbulence in a differentially rotating galactic disk. They estimated the energy input by noting that the energy input from the MRI

$$\dot{e} = T_{r\phi} \Omega, \quad (5)$$

where $T_{r\phi}$ is the Maxwell stress tensor, and Ω the angular velocity. Numerical models by Hawley et al. (1995) suggest that $T_{r\phi} = 0.6B^2/8\pi$, so

$$\begin{aligned} \dot{e} &= (1.2 \times 10^{-28} \text{erg cm}^{-3} \text{s}^{-1}) \times \\ &\times \left(\frac{B}{6 \mu\text{G}} \right)^2 \left(\frac{\Omega}{[220 \text{Myr}]^{-1}} \right). \end{aligned} \quad (6)$$

We can solve equation (4) for the rms velocity that could be powered by this level of energy input, getting $v_{\text{rms}} \sim 4 \text{ km s}^{-1}$, just a little under the typical values observed by Petric & Rupen (2007).

Several groups have now simulated the MRI in galactic disks. Dziourkevitch et al. (2004) did three-dimensional global models with an adiabatic equation of state, and found velocity dispersions varying with height from 1.5 km s^{-1} in the midplane to 3 km s^{-1} at 500 pc and above. Kim et al. (2003); Piontek & Ostriker (2004, 2005) and Piontek & Ostriker (2007) performed a series of models using a shearing box in which they moved from an adiabatic equation of state to the introduction of thermal instability to the inclusion of both thermal instability and vertical stratification. They concluded that the partition of the medium into warm and cold phases was vital to maintaining significant velocity dispersions, with the velocity dispersion in the warm gas ranging from 5 km s^{-1} at the midplane to over 10 km s^{-1} at 500 pc, as shown in Figure 2.

The MRI seems to provide a floor to the possible velocity dispersion in galactic disks. This may explain the success of models that follow gravitational instability in disks of stars and isothermal gas (embedded in dark matter halos), which can reproduce the Schmidt Law (Li et al. 2005a, 2006), and show a tight exponential correlation between the minimum value of the gravitational instability parameter Q_{sg} (Rafikov 2001) and the star formation timescale (Li et al. 2005b).

3. MAGNETIC REGULATION

Aside from driving the MRI, magnetic fields can also directly affect the location and perhaps the rate of star formation in galaxies. Dobbs & Bonnell (2007) computed models without self-gravity of multiphase gas passing through a spiral potential with and without magnetic fields. They found that, without magnetic fields, clear spurs formed along their spiral arms, while with fields having magnetic pressure exceeding the thermal pressure distinct spurs were no longer formed, though some interarm structure remained.

Kim & Ostriker (2006) performed shearing box models of self-gravitating, magnetized gas interact-

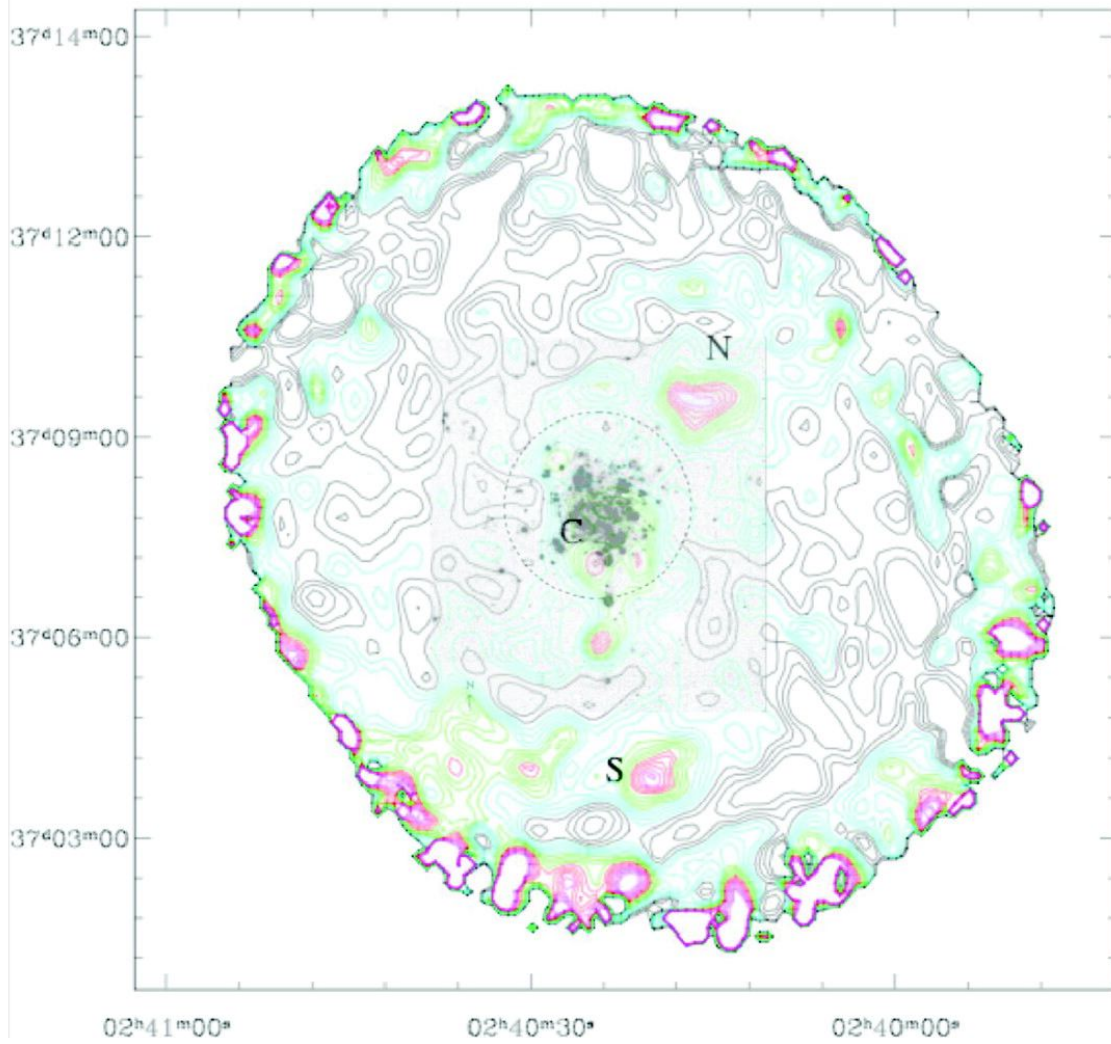


Fig. 1. Distribution of velocity dispersion of HI in the galaxy NGC 1058, overlaid on the $H\alpha$ emission from Ferguson et al. (1998) in greyscale. This demonstrates the surprising uniformity and lack of correlation with star formation of the velocity dispersion. The regions of highest dispersion are labeled N, C, and S. The x and y axis are the RA and Dec in B1950 coordinates. The contours are in km s^{-1} and start in steps of 0.5 km s^{-1} . Black is used for dispersions between 5.5 to 7, cyan for 7.5 to 9, green for 9.5 to 11, red for 11.5 to 13, and magenta for 13.5 to 15 km s^{-1} . From Petric & Rupen (2007).

ing with the fixed stellar potential of a single spiral arm, an approximation appropriate to a disk dominated by stellar mass such as that of the Milky Way. They demonstrated spur formation and gravitational collapse as natural consequences of the interaction of fields with self-gravity, as shown in Figure 4. Shetty & Ostriker (2006) followed up on these models with global two-dimensional models of self-gravitating, magnetized gas in a disk with (and without) an imposed stellar spiral potential, demonstrating the formation of spurs and self-gravitating objects that look likely to form giant molecular clouds and ultimately stellar clusters.

In a magnetized disk, collapse can only occur in regions where the gas accumulation length along field lines is shorter than the generalized Toomre instability length in that region. Cloud formation by such collapse will then lead to the surrounding gas having reduced mass-to-flux ratio, and thus resisting collapse more strongly. This feedback mechanism can be thought of as magnetic regulation of star formation (Shu et al. 2007).

In spiral galaxies, gas accumulation occurs in spiral arms, so the work of Kim & Ostriker (2006) and Shetty & Ostriker (2006) can be used to derive a quantitative estimate of star formation in a magnet-

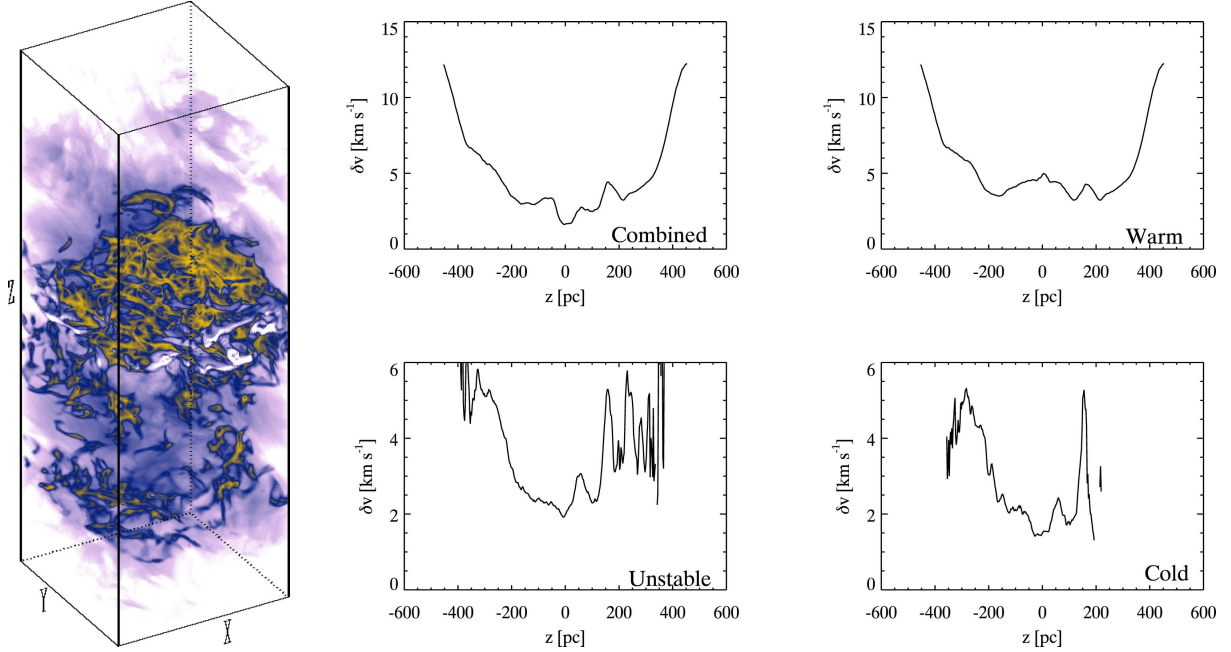


Fig. 2. *Left*: Density in a stratified, two-phase, magnetorotationally unstable disk, computed in a shearing-sheet approximation. *Right*: Vertical profile of mass-weighted velocity dispersion δv for this model for gas within and between the stable thermal phases, as well as for the total gas. From Piontek & Ostriker (2007).

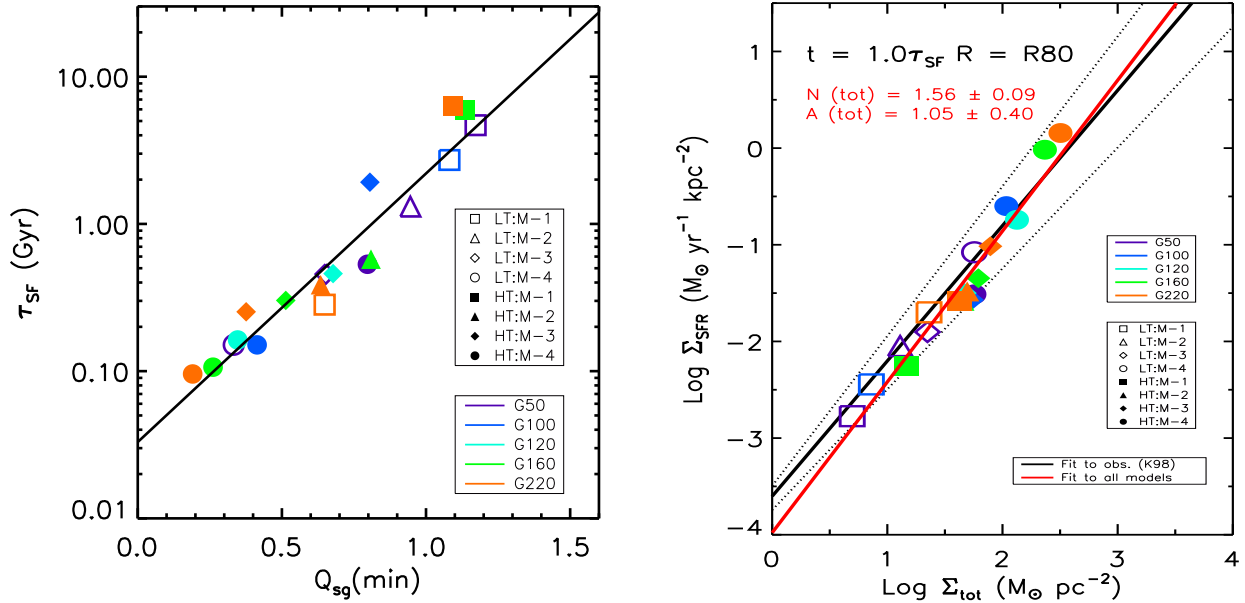


Fig. 3. *Left*: Star formation timescale τ_{SF} correlates exponentially with the initial disk instability Q_{sg} for both low temperature (*open*) and high temperature (*filled*) models. The solid line is a least-squares fit. From Li et al. (2005b). *Right*: A comparison of the global Schmidt laws between simulations from Li et al. (2006) and observations. The red line is the least-square fit to the total gas surface density of the simulated models, the black solid line is the best fit of observations from Kennicutt (1998), while the black dotted lines indicate the observational uncertainty. The color of the symbol indicates the rotational velocity for each model; labels from M-1 to M-4 are sub-models with increasing gas fraction; and open and filled symbols represent low and high temperature models, respectively.

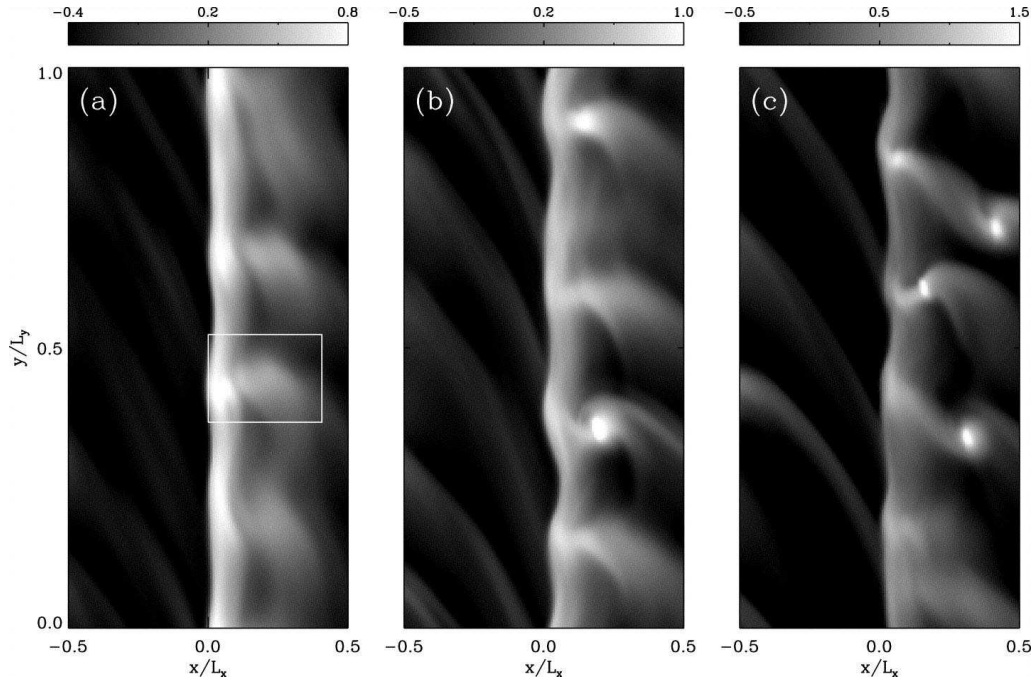


Fig. 4. Surface density ($\log \Sigma/\Sigma_0$ in grey scale) at times of 5.6, 6, and 6.3 orbital times in the magnetized, 3D shearing sheet model of Kim & Ostriker (2006). The scale length for typical parameters is $L_x = L_y/2 = 3.14$ kpc.

ically regulated galaxy. Shu et al. (2007) demonstrate that they can derive a Schmidt Law dependence of the star formation rate on gas surface density from considering spiral arms as example accumulation mechanisms. However, this is a special case for the general question of star formation in galaxies. It remains to be seen whether this mechanism can explain the behavior of irregular galaxies without prominent spiral arms, starburst galaxies, or high-redshift, gas-rich objects.

4. GALAXY FORMATION

Recently the effect of magnetic fields during the galaxy formation era has been directly studied in a preliminary adaptive mesh refinement simulation by Wang & Abel (2009). They studied the collapse of an isolated halo of total mass $10^{10} M_\odot$ initially having an NFW profile (Navarro, et al. 1996). In this first model, further collapse was prevented when the Jeans scale approached the grid scale $\Delta x = 26$ pc, so no mass was transferred to a collisionless population of stars during the evolution of the galaxy. As a result, gravitational stirring of the disk is efficient, maintaining velocity dispersions of 10 km s^{-1} or more, but not from an astrophysically relevant mechanism. Magnetic field was assumed to initially thread the halo with strength of a nanogauss, under the assumption of field production by previous gen-

erations of star formation and active galactic nuclei (e.g. Rees 2006).

The initial evolution of the galaxy shows rapidly increasing amounts of gravitationally unstable gas that ought to produce large numbers of stars in the first several hundred Myr. During this period, the field is amplified in the disk, reaching a few percent of equipartition after about 500 Myr. The field only begins to play a role in supporting the gas after that point, however, while star formation proceeds with little difference between pure hydrodynamic and magnetized models for the entire previous period. The initial conclusion appears to be that even with relatively large initial fields, magnetic effects can be neglected during the initial period of galaxy formation, until a large-scale field has been generated.

5. FIELD GENERATION

This brings us to the question of how such large-scale magnetic fields are formed. Classical Alpha-Omega dynamos require many Gyr to generate observed fields, although somewhat shorter times may be given by a cosmic-ray driven dynamo (see Otmianowska-Mazur, this volume, electronic edition). Turbulent dynamos can generate strong fields much more quickly, but the dominant scale for field structure is then the diffusive scale (Schekochihin et

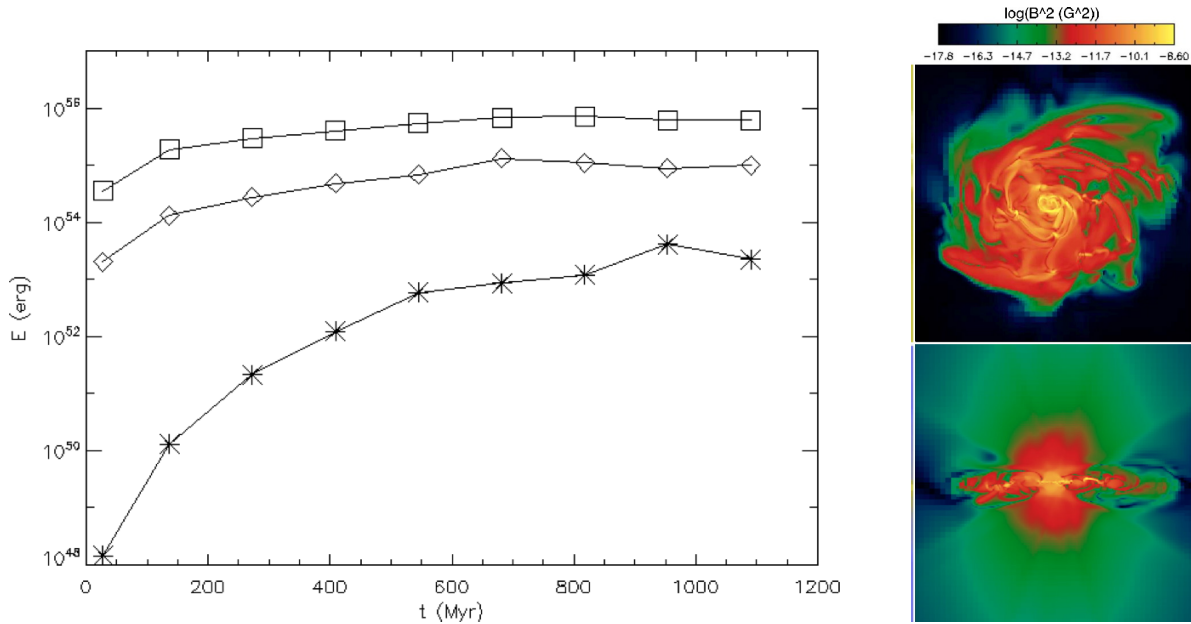


Fig. 5. *Left:* Time history from the AMR model of Wang & Abel (2009) of disk gas kinetic energy (*squares*), thermal energy (*diamonds*), and magnetic energy (*asterisks*), showing the strong growth of magnetic energy over time. *Right:* Horizontal and vertical slices of magnetic pressure after 1.088 Gyr of evolution. The plot square has a side of 11 kpc. From Wang & Abel (2009).

al. 2004), so there is no large-scale, coherent field structure like that observed in galaxies. However, the question of how the tangled field generated by a turbulent dynamo evolves when embedded in a differentially rotating galaxy remains unaddressed.

The simulations I have discussed in this paper do not answer this question, but they do offer suggestive results that might point the way towards the answer. Beginning with the simplest case, we note that the in their stratified, shearing box MRI simulation with thermal instability of Piontek & Ostriker (2007) shows field growth to 3–4 μG in the cold gas within 300 Myr, and then maintains that field strength for another Gyr. Nishikori et al. (2006) performed a three-dimensional, resistive MHD model of a global torus with initially weak azimuthal field threading 10^5 K gas. They found an increase in magnetic energy of eight orders of magnitude over a period of 200 Myr, and then maintain the field at that level for another 600 Gyr.

Wang & Abel (2009) find a similar behavior for the magnetic energy in their simulation of disk formation in a collapsing halo, showing a factor of 10^6 amplification of field energy over 600 Myr, as shown in Figure 5. They further demonstrate that the magnetic field in their disk indeed has large-scale structure after 600 Myr, with several field reversals, clear spiral structure, and field strengths in spiral arms exceeding 10–20 μG (Figure 5).

6. SUMMARY

The major points I have made in this paper are that the MRI may offer a mechanism to maintain a minimum level of turbulence regardless of the strength of star formation. This might then support the picture that gravitational instability acting on disks regulates the strength of star formation in galaxies. The alternative view that magnetic fields regulate star formation appears likely to be valid at least morphologically, but it remains to be seen if the rate of star formation requires magnetic regulation to explain.

A related question is how the large-scale magnetic field in galaxies is generated. Small-scale turbulent dynamos to generate field strength, perhaps with large-scale coherent fields produced at the end by classical dynamo action is an intriguing speculation that remains consistent with the increasingly detailed models that I have reviewed here.

I thank the organizers for their invitation to speak. This work was partly supported by NSF grant AST03-07854 and NASA Origins of Solar Systems grant NNX07AI74G.

REFERENCES

- Balbus, S. A., & Hawley, J. F. 1991, *ApJ*, 376, 214
 _____. 1998, *Rev. Mod. Phys.*, 70, 1

- Dobbs, C. L., & Bonnell, I. A. MNRAS, 374, 1115
- Dziourkevitch, N., Elstner, D., & Rüdiger, G. 2004, A&A, 423, L29
- Elmegreen, B. G. 2002, ApJ, 577, 206
- Ferguson, A., Wyse, R. F. G., Gallagher, J. S., & Hunter, D. A. 1998, ApJ, 506, L19
- Gammie, C. F. 1992, PhD Thesis, Princeton University
- Goldreich, P., & Lynden-Bell, D. 1965, MNRAS, 130, 97
- Hawley, J. F., Gammie, C. F., & Balbus, S. A. 1995, ApJ, 440, 742
- Kennicutt, R. C., Jr. 1998, ApJ, 498, 541
- Kim, W.-T., & Ostriker, E. C. 2006, ApJ, 646, 213
- Kim, W.-T., Ostriker, E. C., & Stone, J. M. 2003, ApJ, 599, 1157
- Kravtsov, A. 2003, ApJ, 590, L1
- Krumholz, M. R., & McKee, C. F. 2005, ApJ, 630, 250
- Li, Y., Mac Low, M.-M., & Klessen, R. S. 2005a, ApJ, 620, L19
- _____. 2005b, ApJ, 626, 823
- _____. 2006, ApJ, 639, 879
- Mac Low, M.-M. 1999, ApJ, 524, 169
- _____. 2003, Lect. Notes Phys., 614, 182
- Martin, C. L., & Kennicutt, R. C., Jr. 2001, ApJ, 555, 301
- Navarro, J. F., Frenk, C. S., & White, S. D. M. 1996, ApJ, 462, 563
- Nishikori, H., Machida, M., & Matsumoto, R. 2006, ApJ, 641, 862
- Petric, A. O., & Rupen, M. P. 2007, AJ, 134, 1952
- Piontek, R. A., & Ostriker, E. C. 2004, ApJ, 601, 905
- _____. 2005, ApJ, 629, 849
- _____. 2007, ApJ, 663, 183
- Rafikov, R. R. 2001, MNRAS, 323, 445
- Rees, M. J. 2006, Astron. Nach., 327, 395
- Schaye, J. 2004, ApJ, 609, 667
- Schekochihin, A. A., Cowley, S. C., Maron, J. L., & McWilliams, J. C. 2004, Phys. Rev. Lett., 92, 084504
- Sellwood, J. A., & Balbus, S. A. 1999, ApJ, 511, 660
- Shetty, R., & Ostriker, E. C. 2006, ApJ, 647, 997
- Shu, F. H., Allen, R. J., Lizano, S., & Galli, D. 2007, ApJ, 662, L75
- Silk, J. 1997, ApJ, 481, 703
- Slyz, A. D., Devriendt, J. E. G., Bryan, G., & Silk, J. 2005, MNRAS, 356, 737
- Toomre, A. 1964, ApJ, 139, 1217
- Wang, P., & Abel, T. 2009, ApJ, 696, 96
- Yang, C.-C., Gruendl, R. A., Chu, Y.-H., Mac Low, M.-M., & Fukui, Y. 2007, ApJ, 671, 374